LEVEL II

AFGL-TR-80-0056

THE ENERGY SPECTRUM OF COSMIC RAY IRON NUCLEI AND THE PREDICTED INTENSITY VARIATION DURING THE SOLAR CYCLE WITH APPLICATIONS FOR THE INTENSITY OBSERVED BY A MAGNETOSPHERIC SATELLITE

W. R. WEBBER
S. M. YUSHAK

Space Science Center
University of New Hampshire
Durham, New Hampshire 03824

November 1979

Final Report
1 May 1979 - 30 September 1979

Approved for public release; distribution unlimited

AIR FORCE GEOPHYSICS LABORATORY
AIR FORCE SYSTEMS COMMAND
UNITED STATES AIR FORCE
HANSCOM AFB, MASSACHUSETTS 01731

409578

80 3 24 011

UNCLASSIFIED

SECURITY CLASSIFICATION OF THIS PAGE (When Data Entered)

REPORT DOCUMENTATION PAGE

READ INSTRUCTIONS BEFORE COMPLETING FORM

1. REPORT NUMBER: 14 AFGL-TR-80-0056	2. GOVT ACCESSION NO.	3. RECIPIENT'S CATALOG NUMBER: 9
4. TITLE (and Subtitle): 6 The Energy Spectrum of Cosmic Ray Iron Nuclei and the Predicted Intensity Variation During the Solar Cycle with Applications for the Intensity Observed by a Magnetospheric Satellite.		5. TYPE OF REPORT & PERIOD COVERED: Final rept. 5/1/79 - 9/30/79
		6. PERFORMING ORG. REPORT NUMBER: 1 May - 30 Sep 79
7. AUTHOR(s): 10 W.R. Webber and S.M. Yushak		8. CONTRACT OR GRANT NUMBER(s): ESD/RADC 79-61
9. PERFORMING ORGANIZATION NAME AND ADDRESS: Space Science Center, University of New Hampshire, Durham, New Hampshire 03824		10. PROGRAM ELEMENT, PROJECT, TASK AREA & WORK UNIT NUMBERS: 62101F 16 7601 17 12 AG
11. CONTROLLING OFFICE NAME AND ADDRESS: Air Force Geophysics Laboratory, Hanscom AFB, Massachusetts 01731, Monitor/D.F. Smart/PHG		12. REPORT DATE: 11 November 1979
		13. NUMBER OF PAGES: 27
14. MONITORING AGENCY NAME & ADDRESS (if different from Controlling Office): 12 27		15. SECURITY CLASS. (of this report): UNCLASSIFIED
		15a. DECLASSIFICATION/DOWNGRADING SCHEDULE

16. DISTRIBUTION STATEMENT (of this Report)

Approved for Public Release; distribution unlimited

17. DISTRIBUTION STATEMENT (of the abstract entered in Block 20, if different from Report)

18. SUPPLEMENTARY NOTES

19. KEY WORDS (Continue on reverse side if necessary and identify by block number)

Cosmic Rays
Radiation dose
Iron Nuclei
Satellite radiation exposure

20. ABSTRACT (Continue on reverse side if necessary and identify by block number)

This report surveys existing measurements of cosmic ray iron nuclei, combines these data and represents them as a function of modulation during a solar cycle. This composite cosmic ray iron nuclei spectrum is then applied to estimate the heavy nuclei flux exposure to a satellite orbiting at 3.5 earth radii taking into account the effects of geomagnetic shielding.

DD FORM 1 JAN 73 1473 EDITION OF 1 NOV 65 IS OBSOLETE

UNCLASSIFIED

SECURITY CLASSIFICATION OF THIS PAGE (When Data Entered)

409578

SECURITY CLASSIFICATION OF THIS PAGE(When Data Entered)

SECURITY CLASSIFICATION OF THIS PAGE(When Data Entered)

THE ENERGY SPECTRUM OF COSMIC RAY IRON NUCLEI AND THE
PREDICTED INTENSITY VARIATION DURING THE SOLAR CYCLE
WITH APPLICATIONS FOR THE INTENSITY OBSERVED BY A MAGNETOSPHERIC SATELLITE

A

ILLUSTRATIONS

TABLES

THE ENERGY SPECTRUM OF COSMIC RAY IRON NUCLEI AND THE PREDICTED INTENSITY VARIATION DURING THE SOLAR CYCLE WITH APPLICATIONS FOR THE INTENSITY OBSERVED BY A MAGNETOSPHERIC SATELLITE

I. INTRODUCTION

The primary galactic cosmic radiation consists approximately of 83% protons, 12% alphas, 1% nuclei of atomic numbers $Z > 2$, and 3% electrons. This radiation is observed to be isotropic, having the same intensity in any direction and extends over an energy range from 10^6 eV to 10^{20} eV. Nuclei heavier than helium comprise only about 1% of the total primary cosmic radiation and have a total integral intensity of about 25 particles/m^2-sec-ster. Cosmic ray nuclei with $Z > 2$ are classified into various charge groups such as L, M, LH and VH. The L-group nuclei include those with $3 \leq Z \leq 5$, the M-group with $6 \leq Z \leq 8$, the LH-group with $9 \leq Z \leq 14$, and the VH-group with $20 \leq Z \leq 28$. The charge group from managanese to nickel, i.e. $25 \leq Z \leq 28$ is commonly referred to as the iron group.

During their travel from the source regions to the vicinity of the earth, the cosmic rays interact with the interstellar medium and generate secondaries. This process is called fragmentation and results in a depletion of the heavy charged primary cosmic rays and production of secondary cosmic rays. The elements H, He, C, O, Ne, Mg, Si, Fe and Ni are present in the cosmic ray sources and the observed abundances at earth deviate less than 20% from the source abundances as a result of the fragmentation in interstellar space (Meyer et al., 1974). The elements N, Na, Al, S, Ar, Ca, Cr and Mn are probably present in the cosmic ray sources but the maj ity of the abundance of these elements observed at earth are due to fragmentation in the interstellar medium. The elements Li, Be, B, F, Cl, K, Si. Ti and V are due almost entirely to fragmentation of higher charged cosmic rays in the interstellar medium and therefore these elements are probably absent in the source regions. Table I shows the relative abundance of the various nuclei observed at earth for energies greater than 0.45 GeV/nucleon (Lezniak and Webber, 1978).

TABLE I

COSMIC-RAY COMPOSITION

CHARGE	>450 MeV/nuc
He	44700 ± 500
Li	192 ± 4
Be	94 ± 2.5
B	329 ± 5
C	1130 ± 12
N	278 ± 5
O	1000
F	24 ± 1.5
Ne	158 ± 3
Na	29 ± 1.5
Mg	203 ± 3
Al	36 ± 1.5
Si	141 ± 3
P	7.5 ± 0.6
S	34 ± 1.5
Cl	9.0 ± 0.6
A	14.2 ± 0.9
K	10.1 ± 0.7
Ca	26 ± 1.3
Sc	6.3 ± 0.6
Ti	14.4 ± 0.9
V	9.5 ± 0.7
Cr	15.1 ± 0.9
Mn	11.6 ± 1.0
Fe	103 ± 2.5
Ni	5.6 ± 0.6

Charged cosmic ray particles are affected by the earth's magnetic field long before they enter the atmosphere. The magnetic field acts as a momentum analyzer. At any point on the earth's surface, primary cosmic rays must have a certain energy in order to arrive at that point from a given direction. A threshold or cutoff rigidity, i.e. the momentum per unit charge ($R_c = cP/Ze$) can be defined at any latitude for particles arriving at a particular zenith and azimuth angle. If the rigidity of the primary particle is equal to or greater than the cutoff rigidity for a given location, then the charged particle can penetrate the geomagnetic field and arrive at the specified location. The equation for determining the cutoff rigidity is $R_c = M \cos^4\lambda/R_e^2 \; [1 + (1-\sin\theta\cos\psi\cos^3\lambda)^{0.5}]^2$, where M is the geomagnetic dipole moment, λ is the geomagnetic latitude, R_e is the earth's radius, θ is the zenith angle and ψ is the azimuthal angle measured from the East. For particles arriving vertically the cutoff rigidity becomes: $R_v = (M \cos^4\lambda)/4R_e^2 = 14.9 \cos^4\lambda$ GV. Vertical cutoff rigidities are high ($\sim$15 GV) near the equator but reduce toward zero at high latitudes and thus the cosmic ray intensity increases at high latitudes. The above approximation for the vertical cutoff rigidity does not allow the deviations of the earth's magnetic field from the dipole model due to the displacement of the geomagnetic center from the geocenter, or for deviations due to magnetic anomalies, or for the actual magnetospheric configuration.

The heavy cosmic rays that arrive at the vicinity of the earth undergo an intensity reduction due to scattering from magnetic irregularities in the interplanetary magnetic field. This intensity reduction is referred to as solar modulation and is observed to be anti-correlated with the 11-year sunspot cycle. The solar modulation is well described by solving numerically a transport equation which incorporates diffusion, convection and adiabatic energy losses of cosmic ray particles during their traversal through the solar wind (Gleeson and Axford, 1968).

In order to describe the solar modulation at different levels of solar activity, it is necessary to know the diffusion coefficient, the solar wind velocity and the outer boundary of the modulating region.

II. ENERGY SPECTRA

1. INTRODUCTION

The differential energy spectra of all cosmic ray nuclei exhibit a spectrum proportional to power laws at high energy; (above $\sim$1 GeV/nuc) $dJ/dT \propto T^{-\gamma}$ where T is the kinetic energy per nucleon and γ is the spectral index. The spectral exponent of secondary cosmic rays are steeper than those of the primaries. This difference in γ between the primary and secondary cosmic rays leads to energy dependent abundance ratios which give information on the confinement and propagation of cosmic rays in the galaxy. The significance of the variation in the spectral exponent for various cosmic ray components has been discussed by Webber et al. (1973) Ormes and Balasubrahmanyan (1973) and Ramaty et al. (1973). Below 1 GeV/nucleon, the differential spectra of cosmic ray nuclei at earth deviate from simple power laws. The differential spectr[illegible]mes flatter with decreasing energy until a maximum in the differential intensity is reached at around a few hundred MeV/nucleon. Below the maximum, the differential intensity decreases monotonically to a few tens of MeV/nucleon.

At the vicinity of this earth, the low energy spectra of the various charges have different shapes and change with time. These changes in the observed spectra are due mainly to the effects of solar modulation.

In the following sections, we will focus our attention on differential energy measurements reported in the literature for the iron charge group. We will discuss the reliability and accuracy of the data and the effects of solar modulation on the iron spectrum.

2. IRON SPECTRA MEASUREMENTS

Figure 1 shows a compilation of the differential energy spectra of iron nuclei for a 7-year period between 1970 and 1977. Changes in the intensity of iron nuclei below 2 GeV/nucleon are due to the effects of solar modulation. The Mt. Washington neutron monitor rate at the time of each measurement is shown on this figure. Also shown on this figure are the calculated iron interstellar spectrum and various modulated spectra. These calculated iron spectra will be discussed later in the text.

The high energy data of Orth et al. (1978) was acquired during a 1972 balloon flight flown in Texas at a ceiling altitude of 5.5 g/cm^2, using a superconducting magnetic spectrometer in conjunction with scintillators and optical spark chambers. The iron spectra was measured in the energy interval between 2 and 150 GeV/nucleon and is known to an accuracy of about ~15% below 5 GeV/nucleon and ~25% above 5 GeV/nucleon.

A low energy measurement of the iron spectrum was obtained by the Chicago group (Garcia Munoz et al., 1975) using satellite and balloon borne instrumentation. The satellite data covered an energy range from 35 to 400 MeV/nucleon and was obtained between May 1973 and December 1973 from the IMP-7 satellite. The IMP-7 telescope measures particle type and energy by using the dE/dx x E technique. The details of the satellite instrumentation has been discussed by Cartwright et al. (1973). The balloon instrumentation consisted of a scintillation-Cerenkov counter telescope giving a charge resolution of 0.4 charge units at iron. The balloon telescope was sensitive to iron nuclei in the energy range from 0.55 to 4 GeV/nucleon. The differential intensity obtained from the balloon data is known to an accuracy of 5-6%. The accuracy of the satellite data varied between 24% at the lowest energy of 35 MeV/nucleon to about 15% at an energy 450 MeV/nucleon.

The measurements of Balasubrahmanyan and Ormes (1973) utilized an ionization spectrometer in conjunction with scintillation and Cerenkov detectors to determine the energy spectra of iron in the energy interval from 2.5 to 25 GeV/nucleon. Their

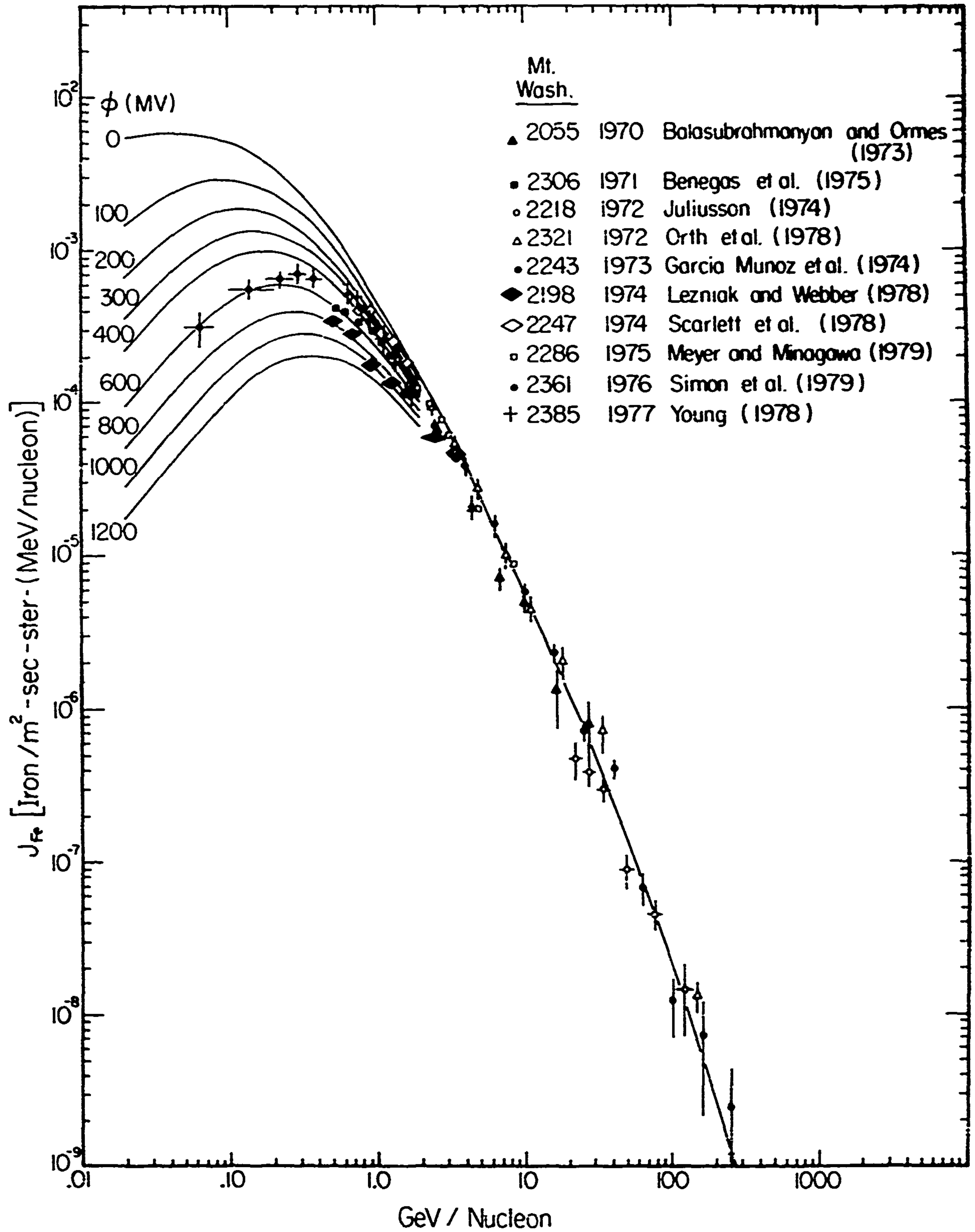

Figure 1. Differential Energy Spectra for Iron Nuclei for the Years 1970-1977.

instrument was flown in New Mexico at a ceiling altitude of 7.4 g/cm^2 for 14.4 hours. The energy is known to an accuracy of 30% between 2.5 and 25 GeV/nucleon. The charge resolution at iron was $\pm$ one charge. The differential iron intensity was measured to an accuracy of about 30%.

The iron spectral measurements of Juliusson (1974) were obtained from three balloon flights between 1971 and 1972 using a scintillation-Cerenkov counter telescope to measure energies between 0.5 and 4 GeV/nucleon and two gas Cerenkov counters for energy measurements between 20 and 100 GeV/nucleon. One flight obtained a ceiling altitude of 4.8 g/cm^2 while two flights obtained an average ceiling altitude of 5.8 g/cm^2. For energies between 20-100 GeV/nucleon the accuracy of the measurements is 20-25%.

The data of Benegas et al. (1975) was obtained with an instrument consisting of a pulsed ionization chamber, a lucite Cerenkov counter and a scintillation counter hodoscope. This instrument had a geometric factor of 0.9 m^2-ster and had a charge resolution of 0.34 charge units at iron. The balloon flight obtained a ceiling altitude of 3.4 g/cm^2. The iron spectrum was measured with high statistical accuracy in the energy interval from about 500 MeV/nucleon to 1.2 GeV/nucleon.

The data of Lezniak and Webber (1978) was obtained using a multi-element balloon-borne telescope consisting of scintillation counters and solid and gas Cerenkov detectors. The instrument was flown at an average ceiling altitude of 2.5 g/cm^2. The iron spectrum was derived from a UVT Cerenkov detector over the energy range from 350 MeV/nucleon to 4 GeV/nucleon. This detector had a charge resolution of 0.4 charge units for Fe. The differential iron intensity was determined with an accuracy of about 7%.

The data of Scarlett et al. (1978) was also obtained from a Cerenkov-scintillation telescope. The balloon reached a ceiling altitude of 2.6 g/cm^2. The iron spectrum was measured over an energy interval from 650 to 1800 MeV/nucleon with an accuracy of about 8%.

The data of Meyer and Minagawa (1977, 1979) was acquired with a balloon-borne scintillation-Cerenkov telescope on two flights which attained an average ceiling altitude of 4.2 g/cm^2. The energy spectra was measured in the energy interval from about 1.4 to 7.5 GeV/nucleon with a reported accuracy of $\leq$7%.

The experiment of Simon et al. (1979) employed an ionization spectrometer and a gas Cerenkov counter to perform two different and independent energy measurements at energies above 10 GeV/nuc. The experiment was flown at an average ceiling altitude of 7 g/cm^2. The iron spectra was measured in the energy interval between 2.5 and 150 GeV/nucleon. For energies less than 25 GeV/nucleon, the accuracy of the measurements is $\lesssim$13%.

The data of Young (1978) is the most recently reported iron spectral measurement. This data was obtained with a balloon-borne instrument consisting of scintillation and Cerenkov counters, a track defining spark chamber and a block of nuclear emulsions. The instrument was flown at a ceiling altitude of 2.6 g/cm^2. The iron spectrum was measured in the energy interval between 600 and 2000 MeV/nucleon, with an accuracy of about 10%.

We can see from Figure 1, the general overall features of the iron spectrum. Below 2 GeV/nucleon the differential spectrum rises to a maximum at an energy $\sim$300 MeV/nuc and falls off at lower energies. The variations in the energy spectra are due to a combination of solar modulation effects and systematic effects due to the different methods of measurement. These systematic effects arise from various corrections necessary to determine the iron intensity at the instrument and at the top of the atmosphere. Above 2 GeV/nucleon the modulation effects have diminished leaving only the systematic variations. Above 2 GeV/nucleon all the data is consistent with a spectral index of 2.3 ± 0.3.

III SOLAR MODULATION EFFECTS AND THE VARIATION OF THE IRON NUCLEI INTENSITY DURING THE SOLAR CYCLE

1. INTRODUCTION

The low energy (<1 GeV/nuc) galactic cosmic rays exhibit intensity variations with an 11-year periodicity. These variations are correlated with solar activity. The sun is observed to go through periods of minimum and maximum solar activity every 11-years. The start of a new solar cycle is characterized by the appearance of sunspots at high latitude on the solar disk. The number of sunspots increases as the cycle progresses and solar activity is observed to increase. Cosmic ray intensity changes at the earth lag the changes in sunspot number by 9 to 12 months. The increase in solar activity modulates the galactic cosmic rays, through the agency of the solar wind, in such a manner that an increase in solar activity corresponds to a decrease in the cosmic ray intensity. From minimum to maximum, the energy density of the primary galactic cosmic rays in the vicinity of the earth decreases by about 40%.

The modulation of cosmic rays by the interplanetary medium is quantitatively determined by a transport equation. The physical model upon which this equation is based represents the solar system as being filled with an expanding fully ionized and highly conducting plasma, the solar wind, which contains frozen-in irregular magnetic fields. Cosmic rays are scattered from these irregularities and execute a random walk in the solar wind. The particles are convected outward by the flow of the solar wind, diffuse inward, and are decelerated by the adiabatic cooling associated with the expansion of the solar wind. The parameters required to define the transport equation and its solution are the diffusion coefficient, which is generally a function of radius and energy, the solar wind velocity and the interstellar energy spectrum.

The basis of current solar modulation theory (Parker, 1965, 1966) is the Fokker-Planck equation for the modulated number density $U(r,T)$ per unit kinetic energy at heliocentric radius r and kinetic energy T. Gleeson and Axford (1967, 1968) have given this equation as

$$\frac{1}{r^2}\frac{\partial}{\partial r}(r^2VU) - \frac{1}{3r^2}\frac{\partial}{\partial r}(r^2V)\frac{\partial}{\partial T}(\alpha TU) - \frac{1}{r^2}\frac{\partial}{\partial r}(r^2K\frac{\partial V}{\partial r}) = 0 \qquad (1)$$

where V is the solar wind velocity and K the effective diffusion coefficient in the interplanetary magnetic field irregularities. The diffusion coefficient is generally a function of $\beta = (v/c)$, magnetic rigidity, R and r. The factor $\alpha = (\gamma+1)/\gamma$, γ being the Lorentz factor $[= 1/(1-\beta^2)^{\frac{1}{2}}]$. Numerical techniques for solving Eq. (1) have been given by Fisk (1971) and Gleeson and Urch (1971). These techniques require the specification of the interstellar density spectrum $U(T_o)$, the functional form of the diffusion coefficient and appropriate boundary conditions. Numerical solutions of Eq. (1) yield the modulated spectra at 1 AU, including the effects of adiabatic deceleration. Adiabatic deceleration can be an important energy loss effect below a few hundred MeV/nucleon (Rygg and Earl, 1971; Goldstein et al., 1970; and Fisk, 1971).

The modulation is described quantitatively by the "modulation parameter", ϕ. This parameter is defined as

$$\phi = \int_r^{R_1} \frac{V}{3K_1(r)}\, dr \qquad (2)$$

where V is the solar wind velocity and $K_1(r)$ is the radial part of the diffusion coefficient. The diffusion coefficient is usually treated as a separable function of radius and rigidity, i.e. $K = \beta\, K_1(r)K_2(R)$.

2. SOLAR MODULATION OF IRON NUCLEI

Figure 2 shows modulated differential iron spectra for various values of the parameter ϕ. The integral intensity of iron nuclei is shown in Figure 3 for similar values of the parameter ϕ. The modulated spectra were obtained by solving the complete transport equation taking into account convection, diffusion and adiabatic deceleration. The interstellar iron spectrum used in the calculations is also shown in Figure 2. This interstellar spectrum, which exists outside the boundary of the

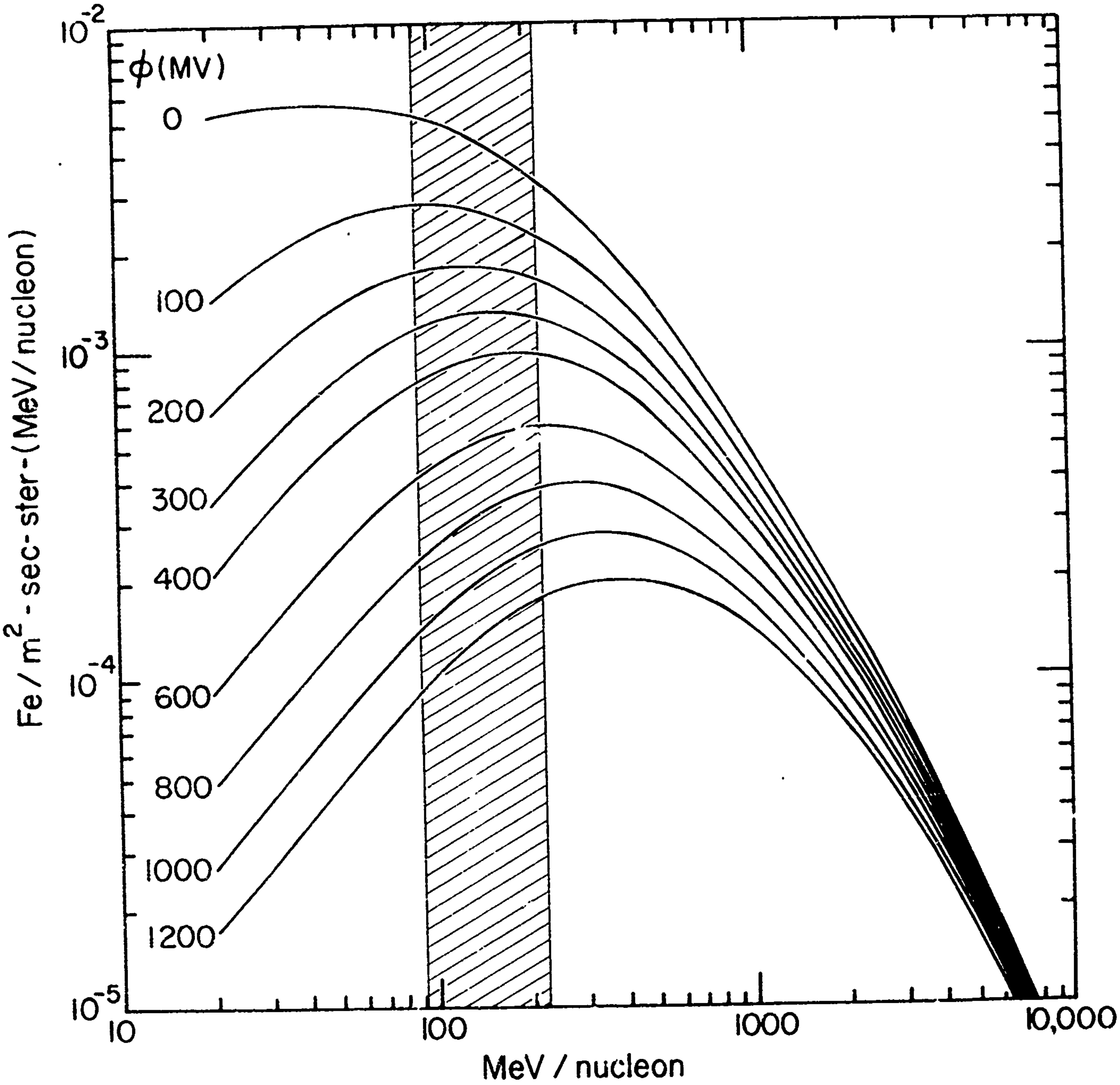

Figure 2. Calculated Differential Intensity of Iron Nuclei for Different Values of the Modulation Parameter ϕ.

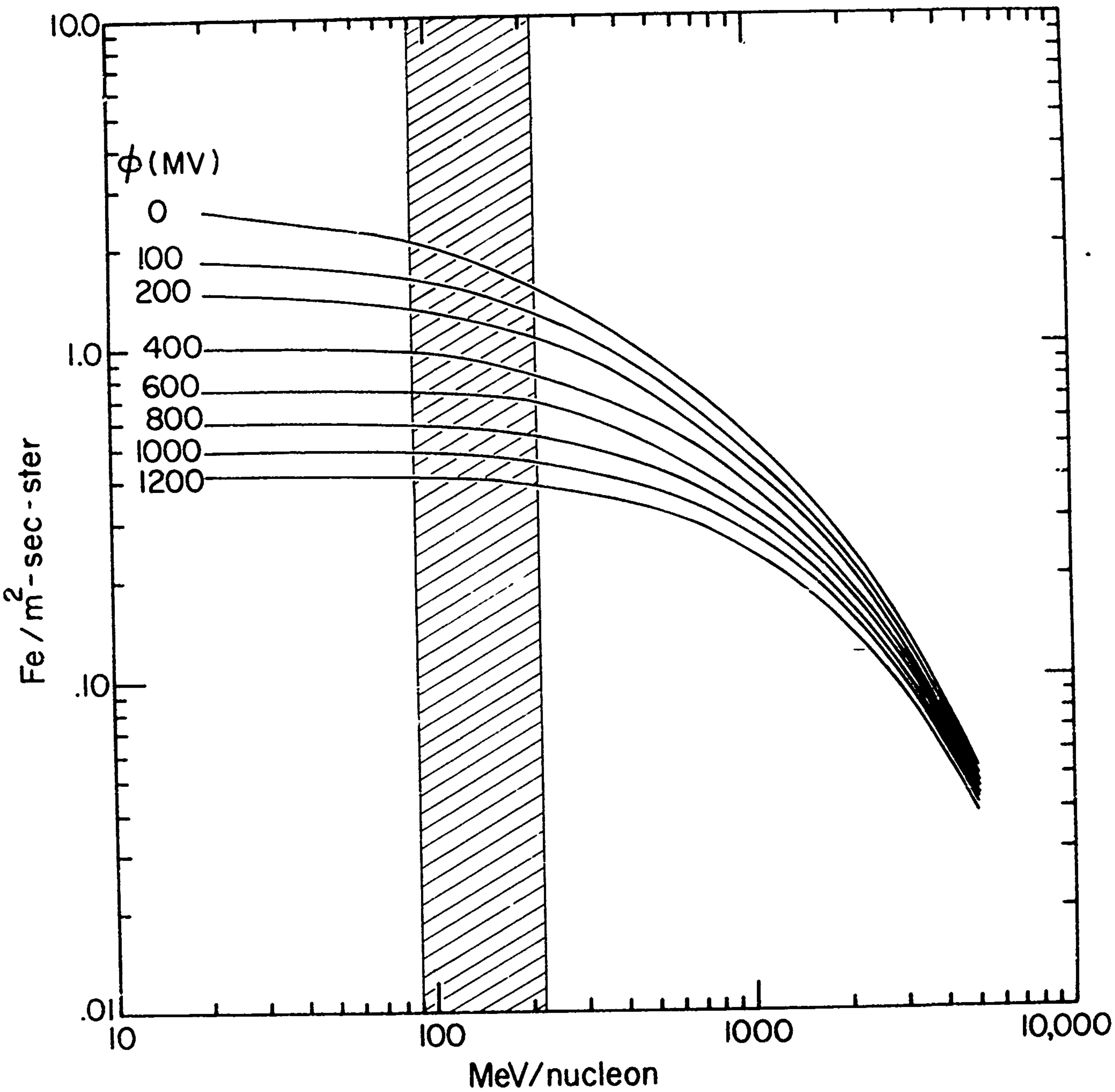

Figure 3. Calculated Integral Intensity of Iron Nuclei for Different Values of the Modulation Parameter ϕ.

modulation region, was chosen from consideration of the much better known modulation of the helium component. The absolute level of modulation has been determined by fitting the measured helium spectrum above using the unique local interstellar helium spectrum deduced by Webber and Yushak, (1979). The curves shown in Figure 2 have also been superimposed in Figure 1.

This procedure is necessary due to the limited number of measurements of the cosmic ray iron spectrum at different levels of solar modulation. There is a lack of data at low energies (<500 MeV/nucleon) where modulation effects are most important. Most measurements as well as theoretical arguments suggest that solar modulation effects on nuclei with the same mass to charge ratio should be the same.

In view of this, it is desirable to estimate the effects of solar modulation on iron nuclei by studying a more abundant cosmic ray component which has a similar mass to charge ratio (A/Z = 2.15 for iron). Helium nuclei (A/Z = 2.0) fulfils both of these requirements and will be used to determine the level of modulation at various times in the solar cycle. The level of solar modulation for helium nuclei can be correlated with the Mt. Washington neutron monitor counting rate and from this correlation, intensity changes in the iron spectrum can be estimated for any level of solar modulation.

Figure 4 shows an example of the measured helium spectra for the years 1965, 1968 and 1969 (Rockstroh, 1977). The calculated modulated spectra are also shown on this figure along with the required interstellar spectrum. Helium nuclei spectra also exist for the years 1970, 1971, 1972, 1974, 1975 and 1977.

The interstellar spectrum shown in Figure 4 was modulated in order to fit the measured helium spectra for each given year. This interstellar spectrum was chosen from a careful study of the abundance ratio $^3He/^4He$ (Webber and Yushak, 1979).

A relationship exists between the modulation parameter ϕ needed to fit the various helium spectra and the Mt. Washington neutron monitor counting rate at the time

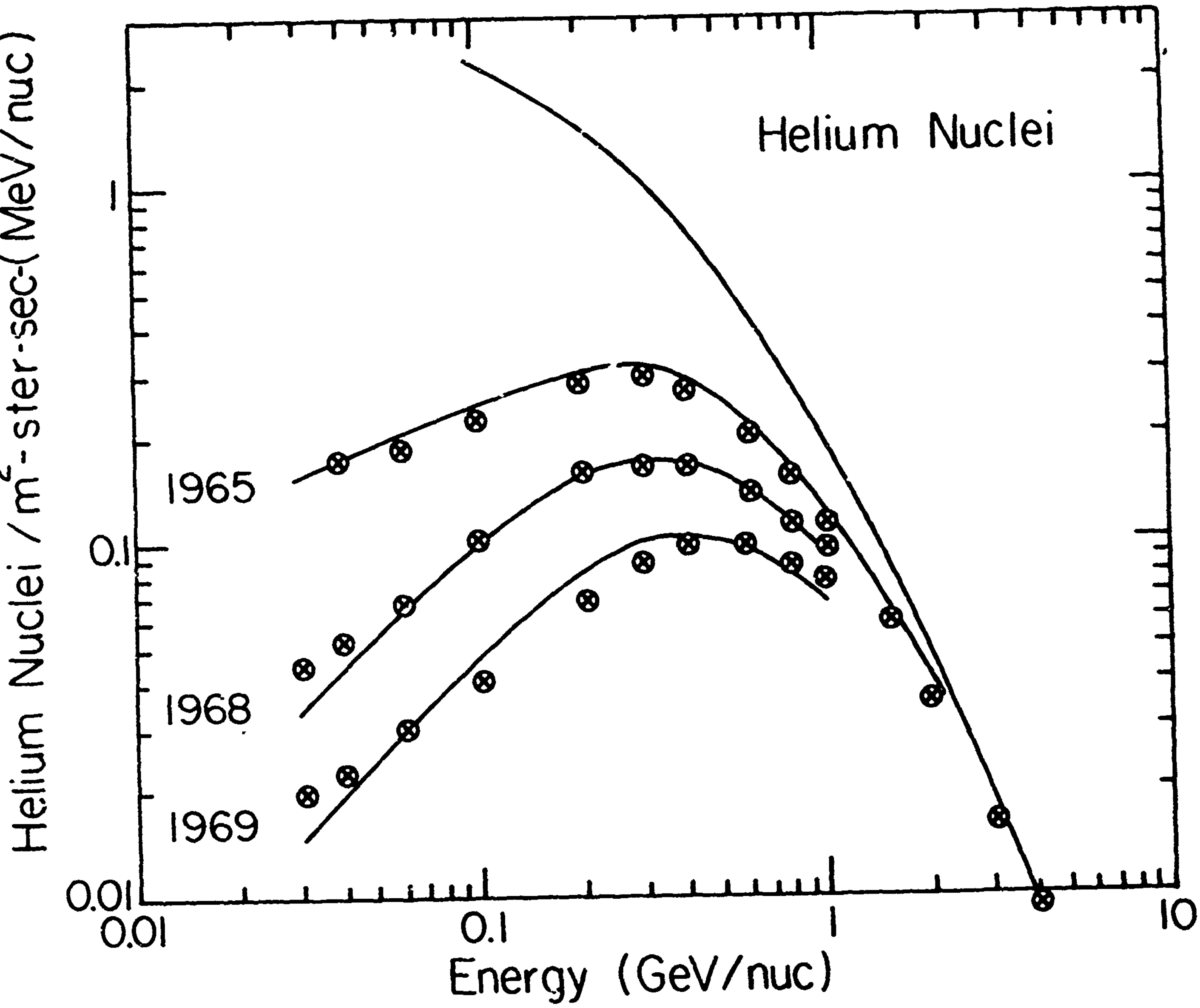

Figure 4. The Measured and Calculated Helium Nuclei for the Years 1965, 1968 and 1969.

of the measurement. This relationship is shown in Figure 5. Note that a ϕ of 400 MV corresponds to sunspot minimum conditions. At this time the maximum flux of cosmic ray particles is seen at earth. The shaded region represents the uncertainty in the correlation of ϕ with the Mt. Washington neutron monitor counting rate. From the curve in Figure 5, the modulation parameter ϕ for iron nuclei can be determined for any given Mt. Washington neutron monitor counting rate. Once ϕ is determined, the iron nuclei integral and/or differential intensity at any energy can be obtained from Figure 2 or Figure 3.

IV. VERTICAL CUTOFF RIGIDITY FOR IRON NUCLEI IN THE EARTH'S MAGNETOSPHERE

1. INTRODUCTION

All charged cosmic ray nuclei entering the earth's magnetosphere are subject to magnetic forces which alters their trajectories. The result of this field-particle interaction manifests itself as a rigidity dependent effect in which cosmic ray particles must have a certain threshold rigidity in order to arrive at any given location on the earth's surface. This effect varies with the latitude, λ, of observation and with the viewing direction (i.e. zenith angle, θ and azimuth angle, ψ). The equation for determining the cutoff rigidity is:

$$R_c = M \cos^4\lambda/R_e^2 \ [1 + (1-\sin\theta\cos\psi\cos^3\lambda)^{0.5}]^2 \tag{3}$$

where M is the geomagnetic dipole moment, λ is the geomagnetic latitude, R_e is the earth's radius, θ is the zenith angle and ψ is the azimuthal angle measured from the East. For particles arriving vertically the cutoff rigidity becomes:

$$R_v = (M \cos^4\lambda)/4R_e^2 = 14.9 \cos^4\lambda \text{ GV} \tag{4}$$

The verticle cutoff rigidity is defined as the minimum rigidity for which cosmic ray particles can arrive at : particular location from the zenith. Vertical cutoff rigidities are highest at the equator and reduce toward zero at the poles, thus the cosmic ray intensity increases at high latitudes. Cutoff rigidities are lower

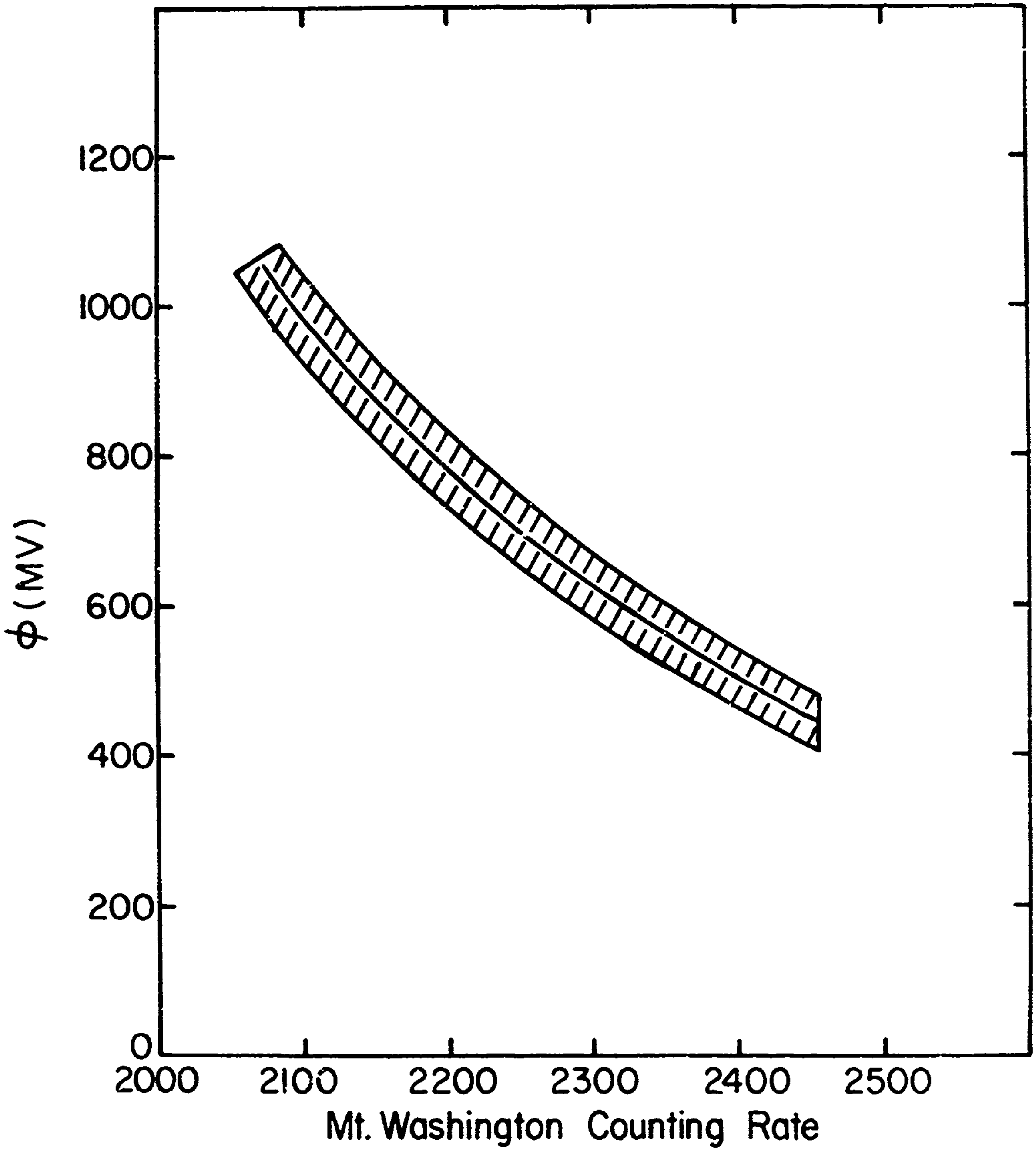

Figure 5. The Modulation Parameter ϕ Versus Mt. Washington Neutron Monitor Counting Rate.

when viewing toward the West than when viewing toward the East. This East-West effect becomes more predominate as the latitude decreases.

Various attempts have been made to model the earth's magnetic field and compute particle trajectories and cutoff rigidities. The earliest attempts calculated particle trajectories and cutoff rigidities in the earth's equatorial plane by assuming that the earth's magnetic field could be represented as a geocentric dipole. Discrepancies between calculated and measured cosmic ray intensities resulted because of the non-dipole character of the earth's magnetic field. The magnetic center is displaced from the geocenter by about 436 km.

Shea et al. (1965, 1967a, 1975) have used a "trajectory tracing technique" to determine the vertical cutoff rigidity at a number of locations on the earth's surface. This method uses a model for the geomagnetic field representation and for a given rigidity particle traces its orbit outward from a given latitude, longitude and altitude in a given direction to see whether or not it escapes the earth's magnetosphere.

A coordinate system based on the McIlwain (1961) parameters B and L has been found useful for ordering cosmic ray data. The parameter L is defined through the relationship $L = R_m \cos^2 \lambda_m$ where R_m is the distance from the effective magnetic center in earth radii and λ_m is the effective magnetic latitude. The B - L coordinate system essentially restores dipole symmetry to the earth's magnetic field.

By using the relationship $1/L = \cos^2 \lambda_m / R_m$ the equation for the vertical cutoff rigidity becomes: $R_v = R_o L^{-2}$. Shea and Smart (1967b) have determined that the best fit to the cosmic ray data for the vertical cutoff rigidity in L-coordinates is; $R_v = 15.96\ L^{-2.0005}$.

2. VERTICAL CUTOFF RIGIDITIES FOR IRON NUCLEI AT SATELLITE ALTITUDES IN THE EQUATORIAL PLANE

Consider a hypothetical earth satellite orbiting in an equatorial orbit at a distance h above the earth's surface. The vertical cutoff at altitude h can be determined if the cutoff near the surface is known. The vertical cutoff rigidity at altitude h is related to the surface cutoff rigidity viz. $R_h = R_{surface} L^{-2}$ (Shea and Smart, 1967b), where L is the appropriate value of the L-coordinate at altitude h.

In order to determine the cutoff rigidity, for example, at 3.5 earth radii over the equator, the cutoff rigidity at the surface must be known. This can be obtained from the five by fifteen degree world grid of trajectory-derived vertical cutoff rigidities given by Shea and Smart (1975). A satellite in an orbit above the geographic equator sweeps through a ±10° band in geomagnetic latitude about the magnetic equator. The vertical cutoff rigidity extremes at the surface in this latitude range go from 11.07 GV to 17.67 GV. At 3.5 earth radii, therefore, the vertical cutoff rigidity varies between .90 and 1.44 GV. This band of vertical cutoff rigidities is shown as a shaded region in Figure 2 and 3. At energies below the cutoff band, iron nuclei are excluded from the satellite.

V. APPLICATIONS

The purpose of this section is to quantitatively estimate the omnidirectional flux of iron nuclei that would be seen by a 4π detector aboard an equatorial satellite orbiting at about 3.5 earth radii. The "view" of a detector on such a satellite would be obstructed by the presence of the solid earth. The fraction of the total solid angle which is obstructed depends essentially on the altitude of the satellite.

The cutoff rigidity in the direction of local West at the satellite will be a minimum, i.e. it will be less than the vertical cutoff rigidity thereby allowing particles with energy below the vertical cutoff rigidity to be observed by the detectors in the satellite. The cutoff rigidity observed in the direction of local East will be higher than the vertical cutoff rigidity.

The solid angle subtended by the earth at a satellite orbiting at 3.5 earth radii is calculated to be 0.16π steradians. This value is obtained from the equation $\Omega = 2\pi \int_0^{\theta} \sin\theta d\theta$ where θ is the polar angle subtended by the earth in a local spherical coordinate system. In the calculations, the earth's radius is assumed to be 1.5 times its actual radius to account for shielding effects of the atmosphere and the magnetic field. Thus, an omnidirectional detector will have an effective solid angle of unobstructed view of about 3.84π steradians.

In order to obtain an estimate of the cutoff rigidity that would be observed in the direction of local East and local West at the satellite, we use the Störmer (1955) equation in the following form:

$$R(\theta,\psi) = \frac{4R_V}{[1 + (1-\sin\theta\cos\psi\cos^3\lambda)^{\frac{1}{2}}]^2} \qquad (5)$$

where θ is the zenith angle, ψ is the azimuth angle measured clockwise from the East, λ is the geomagnetic latitude and R_V is the known vertical cutoff at the altitude of the satellite. Using Eq. (5), the ratio of the cutoff rigidity in the direction of local West to the cutoff rigidity in the vertical direction is: $R(\text{West})/R_V = 0.686$.

The ratio of the cutoff rigidity in the direction of local East to the cutoff rigidity in the vertical direction is: $R(\mathrm{East})/R_V = 4.0$.

In order to determine the integral omnidirectional flux of iron nuclei at the satellite, it is necessary to determine an effective average cutoff rigidity. It has been shown that the cutoff rigidity varies from 0.686 R_V in the West to $4R_V$ in the East. An average cutoff rigidity was determined by using Eq. (5) to calculate the cutoff rigidity at the center of a series of boxes spanning 10° in zenith angle and 30° in the azimuth angle. The calculated cutoff rigidity for each box was weighted by the fraction of the total solid angle subtended by each box at the satellite. The result of the calculation indicates that the effective average cutoff rigidity is about $1.1R_V$.

The vertical cutoff rigidity was calculated to be between 0.90 and 1.44 GV. Using these values, the effective average cutoffs lies between a lower bound cutoff of 0.99 GV and an upper bound cutoff of 1.58 GV. These cutoff values correspond to energies of 107 and 255 MeV/nucleon respectively. Table 2 presents the integral omnidirectional flux of iron nuclei for both the lower bound and the upper bound cutoff as a function of the modulation parameter ϕ.

TABLE 2

INTEGRAL OMNIDIRECTIONAL IRON NUCLEI FLUX

VERSUS MODULATION PARAMETER ϕ

MODULATION PARAMETER ϕ (MV)	IRON FLUX (Fe/m^2-sec) Lower Bound Cutoff	Upper Bound Cutoff
400	3.6	2.9
600	2.8	2.5
800	2.3	2.0
1000	1.8	1.7
1200	1.6	1.4

VI. REFERENCES

Balasubrahmanyan, V. K., and Ormes, J. F., 1973, Astrophys. J., 186, 109.

Benegas, J. C., Israel, M. H., Klarmann, J., and Maehl, R. C., 1975, Proc. 14th International Cosmic Ray Conf., Munich, 1, 251.

Cartwright, B. J., Garcia-Munoz, M., and Simpson, J. A., 1973, Proc. 13th International Cosmic Ray Conf., Denver, 1, 232.

Fisk, L. A., 1971, J. Geophys. Res., 76, 221.

Garcia-Munoz, M., Juliusson, E., Mason, G. M., Meyer, P., and Simpson, J. A., 1975, Astrophys. J., 197, 489.

Gleeson, L. J., and Axford, W. I., 1967, Astrophys. J., 149, L115.

Gleeson, L. J., and Axford, W. I., 1968, Astrophys. J., 154, 1011.

Gleeson, L. J., and Urch, I. H., 1971, Astrophys. Space Sci., 11, 288.

Goldstein, M. L., Fisk, L. A., and Ramaty, R., 1970, Phys. Rev. Letters, 25, 832.

Juliusson, E., 1974, Astrophys. J., 191, 331.

Lezniak, J. A., and Webber, W. R., 1978, Astrophys. J., 223, 676.

McIlwain, C. E., 1961, J. Geophys. Res., 66, 3681.

Meyer, P., Ramaty, R., and Webber, W. R., 1974, Physics Today, 27, 23.

Meyer, P., and Minagawa, G., 1977, Proc. 15th International Cosmic Ray Conf. Plovdiv, 1, 249.

Meyer, P., and Minagawa, G., 1979, Proc. 16th International Cosmic Ray Conf., Kyoto, 1, 329.

Ormes, J. F., and Balasubrahmanyan, V. K., 1973, Nature, 241, 95.

Orth, C. D., Buffington, A., Smoot, G. F., and Mast, T. S., 1978, Astrophys. J., 226, 1147.

Parker, E. N., 1965, Planet Space Sci., 13, 9.

Parker, E. N., 1966, Planet Space Sci., 14, 371.

Ramaty, R., Balasubrahmanyan, V. K., and Ormes, J. F., 1973, Science, 180, 731.

Rockstroh, J. M., 1977, Ph.D. Thesis (University of New Hampshire).

Rygg, T. A., and Earl, J. A., 1971, J. Geophys. Res., 76, 7445.

Scarlett, W. R., Freier, P. S., and Waddington, C. J., 1978, Astrophys. Space Sci., 59, 301.

Shea, M. A., and Smart, D. F., 1965, J. Geophys. Res., 70, 4117.

Shea, M. A., and Smart, D. F., 1965a, J. Geophys. Res., 72, 2021.

Shea, M. A., and Smart, D. F., 1967b, J. Geophys. Res., 72, 3447.

Shea, M. A., and Smart, D. F., 1975, Proc. 14th International Cosmic Ray Conf., Munich, 4, 1298.

Simon, H., Spiegelhaver, H., Schmidt, W. K. H., Siohan, F., Ormes, J. F., Balasubrahmanyan, V. K., and Arens, J. F., 1979, submitted to Astrophys. J.

Störmer, C., 1955, The Polar Aurora, Oxford University Press.

Webber, W. R., Lezniak, J. A., Kish, J. C., and Damle, S. V., 1973, Nature, 241, 96.

Webber, W. R., and Yushak, S. M., 1979, Proc. 16th International Cosmic Ray Conf., Kyoto, 1, 383.

Young, S. M., 1978, Ph.D. Thesis (University of Minnesota).